Method of calculating the alignment tolerance of a Porro prism resonator

Jyh-Fa Lee and Chung Yee Leung

A method of calculating the angular alignment tolerance of a Porro prism laser oscillator is presented. The reduction in mode volume due to misalignment is found by a ray optical approach. An analytical expression for alignment tolerance, in terms of resonator length L, prism azimuth angle θ, rod location L_2, and rod aperture radius a is obtained. An experiment was set up to measure the laser output reduction due to reflector tilting. Results obtained are in good agreement with the theoretical predictions.

I. Introduction

The Porro prism resonator, formed with two crossing Porro prism end reflectors facing each other and an intracavity polarizing beam splitter as output coupler, has two major advantages. First, its output coupling ratio can be continuously tuned by varying the prism azimuth angle.[1] Second, it is less sensitive to misalignment compared with conventional resonators.[2,3] Due to these advantages, this type of resonator is widely used where easy adjustment of laser power during assembly or maintenance, and stability during field operation are important concerns.

In previous work, the operational characteristics of the Porro prism laser resonator, such as variable outcoupling, extinction ratio, and prelasing boundaries, have been analyzed.[1] It has been proved that this type of resonator is relatively insensitive to misalignment in one direction.[2] We have recently studied the pointing direction changes and lateral displacements of the laser beam in a Porro prism resonator due to angular misalignment[4,5]; however, its output energy decay due to misalignment has not been studied in detail. There is, thus, a need for a theoretical model which allows laser design engineers to calculate the alignment tolerance of the Porro prism resonator.

Generally, the alignment tolerance of a resonator formed with two plane or spherical mirrors is found by calculating the field distribution in the resonator and the diffraction loss caused by misalignment.[6–8] However, since the Porro prism resonator is not circularly symmetric, field distribution calculations are complicated.

In this paper, we use a ray optics method to analyze the effect of angular misalignment on the output reduction of the Porro prism oscillator. Analytical expressions for output decay and alignment tolerance in terms of resonator length, prism azimuth angle, rod location, and the rod radius are obtained. An experiment was set up to measure the output energies and the alignment tolerances. Results obtained are in good agreement with our theoretical predictions.

II. Model for Calculating Alignment Tolerance

In this section, the effect of misaligning an end reflector of a Porro prism laser resonator on its output is analyzed using ray optics theory. A model for alignment tolerance calculation is introduced. The alignment tolerance of a laser oscillator is generally defined as the misalignment angle leading to 50% output reduction.

The top view of a misaligned Porro prism resonator with an intracavity polarizing beam splitter as output coupler is shown in Fig. 1. In our analysis, prism 1 is taken to be in perfect alignment while prism 2 is tilted in the horizontal (y) direction. The angle between the axis of the prism 2 and the original optical (z) axis is β, which is positive when the axis of the Porro prism is rotated clockwise from the z axis. The apex orientations of the Porro prisms looking back from P are illustrated in Fig. 2, where AB and CD are the apexes of the prism 1 and prism 2, respectively. Points O and P are the apex centers. The angle between the apex and the y axis is defined as the prism azimuth angle θ. For our laser, the azimuth angle of prism 2 is fixed at 0°,

The authors are with National Central University, Institute of Electro-Optical Science, Chung-Li, Taiwan 32054, China.
Received 1 February 1989.
0003-6935/89/173691-07$02.00/0.

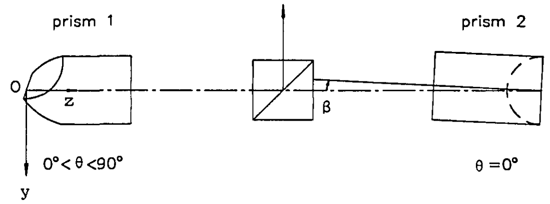

Fig. 1. Top view of a Porro prism resonator angular misaligned in the horizontal direction (β is positive).

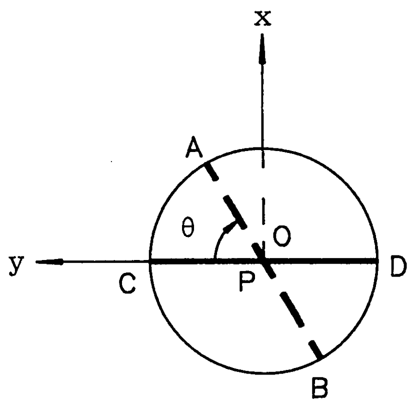

Fig. 2. Apex orientations of the two Porro prisms.

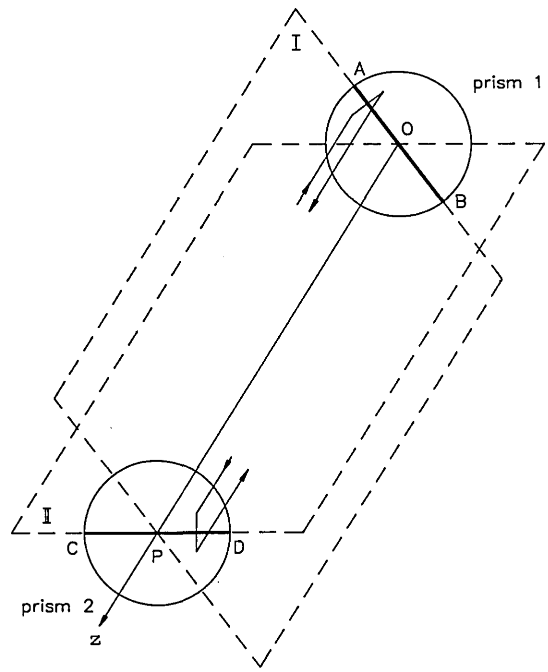

Fig. 3. Conceptual picture of the apex planes of a perfectly aligned Porro prism resonator.

while the azimuth angle of prism 1 is varied from 0° to 90° to tune its output coupling ratio.

The mode axis of a resonator is generally defined as the central axis of the resonating modes. In the ray optics picture, this is the central axis of the bundle of oscillating stable rays. When the resonator is optimally aligned, the mode axis coincides with the z-axis, which is also the central axis of the laser rod. Assuming the apertures of the end reflectors are larger than that of the laser rod, every stable ray must be parallel to the z-axis and must have ray height within the laser rod aperture. Thus the mode area equals the rod aperture area. The ray height here is defined to be the radial distance of the ray path from the mode axis.

For the perfectly aligned Porro prism resonator we may define two apex planes, each containing the apex of one prism, making an equal angle (45°) with the corresponding roofs. This is illustrated in Fig. 3, in which I is the apex plane of prism 1 and II is the apex plane of prism 2. The intersection of these two planes ($\overline{OP}$) defines the mode axis; this can be clearly visualized from the following argument. For a ray parallel to the mode axis incident at Porro prism 1, the ray path of the exiting ray is the mirror image of the incident path in plane I (see Fig. 3) due to the single-axis retroreflecting property of the Porro prism. Similarly, any incident ray parallel to the z-axis will be returned by prism 2 in a path that is the mirror image of the incident path in plane II. Careful analysis reveals that the axial distance of a given ray is not changed by reflections at the Porro prisms, while its path oscillates over a cylindrical surface coaxial with the mode axis.

When prism 2 is angularly misaligned in the horizontal (y) direction, the apex planes are also tilted and no longer make equal angles with the corresponding roofs. The tilted angles are $\beta \csc\theta$ (I) and $\beta \cot\theta$ (II) compared with the original apex planes (see the Appendix). The intersection of the two planes becomes $\overline{P'Q'}$, which is the new mode axis.[5] As depicted in Figs. 4 and 5, the new mode axis passes through the laser medium along $\overline{R'S'}$, which is shifted from the rod axis $\overline{RS}$. Since the path of every oscillating ray describes a cylindrical surface coaxial with the mode axis in the way described above, the mode volume is reduced due to the mode axis displacement. The mode area now has a radius given by the distance from the new mode axis to the nearest edge of the laser medium aperture, as illustrated in Figs. 4 and 5. Figure 6 is a spot diagram of the misaligned resonator showing the ray positions of an oscillating ray. The numbers indicate the sequence of position hopping due to reflections; the ray positions describe a circle with $P'(Q')$ as its center.

Let us denote the radial displacements of the mode axis at prism 1, both ends of the laser rod, and prism 2 by Δ_1, Δ_2, Δ_3, and Δ_4, respectively. These displacements can be expressed as (taken from our recent paper[5])

$$\begin{aligned}
\Delta_1 &= \overline{OQ'} \cong L\beta \cot\theta \csc\theta,\\
\Delta_2 &= \overline{RR'} \cong \beta \csc\theta (L^2 \cot^2\theta + L_1^2)^{1/2},\\
\Delta_3 &= \overline{SS'} \cong \beta \csc\theta (L^2 \cot^2\theta + L_2^2)^{1/2},\\
\Delta_4 &= \overline{PP'} \cong L\beta \csc^2\theta,
\end{aligned} \tag{1}$$

where L is the resonator length, $L_1 = \overline{OR}$ and $L_2 = \overline{OS}$, R and S are the centers of the end apertures of the rod, while R' and S' are the points where mode axis intersects the end surfaces of the rod, as shown in Figs. 4 and 5. It should be noted here that the allowed misalign-

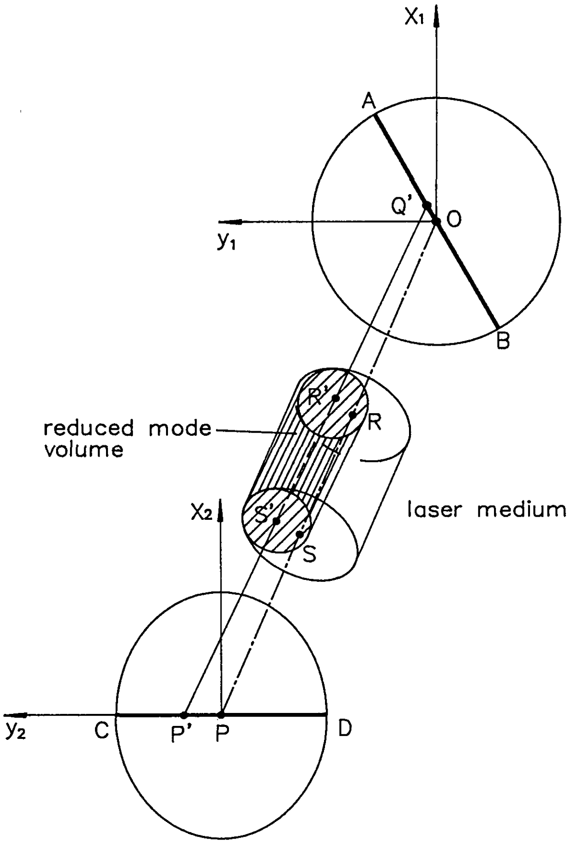

Fig. 4. Location of the tilted mode axis in a misaligned Porro prism resonator (end view).

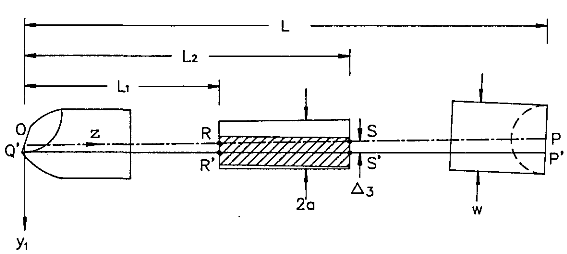

Fig. 5. Location of the tilted mode axis in a misaligned Porro prism resonator (top view).

ment angle in practice are much smaller than those shown in these figures; this allows us to take small angle approximations in our theoretical calculations in this paper. The shadowy regions in Figs. 4 and 5 represent the reduced mode volume in the active medium for the misaligned resonator. It is a cylindrical rod of radius $r = a - \Delta_3$, where a is the actual radius of the laser rod.

For a simplified treatment, we assume the photon density distribution inside the mode volume to be uniform. The laser output energy can then be regarded as proportional to the cross section of the mode volume in the same pumping conditions. Under this assumption, the normalized output energy of a misaligned Porro prism laser oscillator can be written as

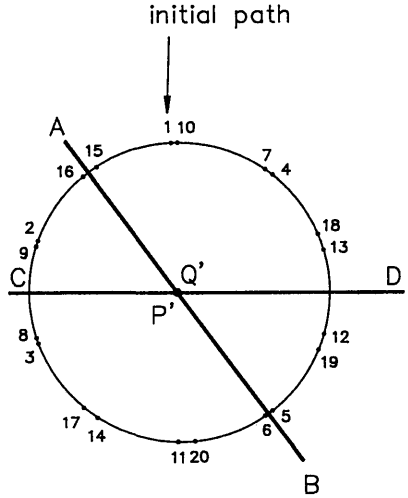

Fig. 6. Spot diagram of the path positions of an oscillating ray.

$$E(\beta)_{\text{nor}} = \frac{E(\beta)}{E(0^\circ)} \cong \frac{\pi(a-\Delta_3)^2}{\pi a^2} = \left(1 - \frac{\Delta_3}{a}\right)^2 . \tag{2}$$

In the above expression, $E(0^\circ)$ and $E(\beta)$ are the output energies of the optimally aligned, misaligned resonators, respectively. Substituting Δ_3 in Eq. (1) into Eq. (2), we get

$$E(\beta)_{\text{nor}} \cong \left[1 - \frac{\beta \csc\theta (L^2 \cot^2\theta + L_2^2)^{1/2}}{a}\right]^2 . \tag{3}$$

For the quantities Δ_3 and β in Eqs. (2) and (3), we take their absolute values.

The alignment tolerance in the horizontal direction is defined as the misalignment angle that causes 50% reduction of the output energy and is denoted by $\beta_{1/2}$. Then Eq. (3) becomes

$$\frac{1}{2} \cong \left[1 - \frac{\beta_{1/2} \csc\theta (L^2 \cot^2\theta + L_2^2)^{1/2}}{a}\right]^2 . \tag{4}$$

The alignment tolerance in the horizontal direction can be expressed as

$$\beta_{1/2}(\theta) \cong \frac{0.293 a \sin\theta}{(L^2 \cot^2\theta + L_2^2)^{1/2}} . \tag{5}$$

Equation (5) gives directly the alignment tolerance in the horizontal direction, which is a function of the prism azimuth angle, the resonator length, the rod diameter, and the longitudinal location of the laser rod inside the cavity. The above equation has been deduced without considering the refractive effect of the laser medium. To obtain a more precise expression, the refractive effect of the rod itself should be taken into account. In this case, Δ_3 in Eq. (1) must be modified (taken from our previous paper[5])

$$\begin{aligned}\Delta_3 \cong \beta \Bigg\{ & \left[L - d\left(1 - \frac{1}{n}\right)\right]^2 \cot^4\theta \\ & + 2\left[L - d\left(1 - \frac{1}{n}\right)\right]\left[L_2 - d\left(1 - \frac{1}{n}\right)\right] \cot^2\theta \\ & + \left[L_2 - d\left(1 - \frac{1}{n}\right)\right]^2 + (L - L_2)^2 \cot^2\theta \Bigg\}^{1/2} ,\end{aligned} \tag{6}$$

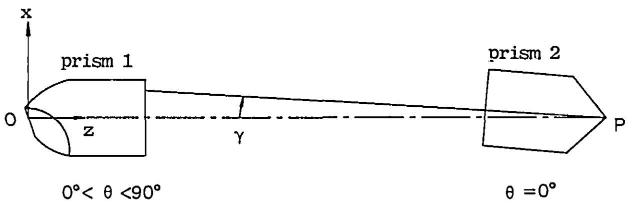

Fig. 7. Porro prism resonator angularly misaligned in the vertical direction.

where d and n are the length and the refractive index of the laser rod, respectively.

Substituting Eq. (6) into Eq. (2) and after similar manipulations, the normalized output energy and the alignment tolerance become

$$E(\beta)_{\text{nor}} \cong \left[1 - \frac{\beta H(\theta)}{a}\right]^2, \tag{7}$$

$$\beta_{1/2}(\theta) \cong \frac{0.293a}{H(\theta)}, \tag{8}$$

where

$$H(\theta) \cong \left\{\left[L - d\left(1 - \frac{1}{n}\right)\right]^2 \cot^4\theta + 2\left[L - d\left(1 - \frac{1}{n}\right)\right]\left[L_2 - d\left(1 - \frac{1}{n}\right)\right]\cot^2\theta + \left[L_2 - d\left(1 - \frac{1}{n}\right)\right]^2 + (L - L_2)^2 \cot^2\theta\right\}^{1/2}. \tag{9}$$

It is worth mentioning that Eqs. (5) and (8) are valid for

$$\frac{\Delta_3}{2a} > \frac{\Delta_4}{W},$$

where W is the diameter of the Porro prism aperture. This situation is met in most practical Porro prism resonators, since W is usually twice as large as $2a$ and Δ_4 is only slightly larger than Δ_3. If the above condition is not valid, the alignment tolerance is determined by the Porro prism aperture instead of the laser rod aperture.

So far, we have analyzed the output energy degradation due to horizontal misalignment. What happens if prism 2 is tilted in the vertical (x) direction instead? This situation is shown in Fig. 7, where γ is the angle of misalignment in the vertical direction. We had theoretically and experimentally proved that the mode axis in this situation is always identical to the original mode axis of a perfectly aligned resonator. Misalignment in the vertical direction does not lead to any lateral displacement of the mode axis and consequently does not cause any reduction of the output energy according to our above arguments. This result is expected from the retroreflecting properties of the Porro prism.

III. Experimental Studies

An experiment is set up to measure the output energy reduction due to angular misalignment. Figure 8 is a sketch of the pulsed Nd:YAG laser oscillator used. Porro prism 2 is mounted on a rotary stage in which a micrometer screw is used to control the misalignment angle β in the horizontal direction. Prism 1 is angularly adjusted to $\theta = 60°$. In the beginning, the oscillator is optimally aligned by monitoring the output pattern and energy. Then prism 2 is tuned to $\beta = 2$ min of arc and the output pulse energy is recorded. This procedure is repeated by increasing the misalignment angle 2 min of arc each time. The same experimental procedure is repeated for $\theta = 30°$.

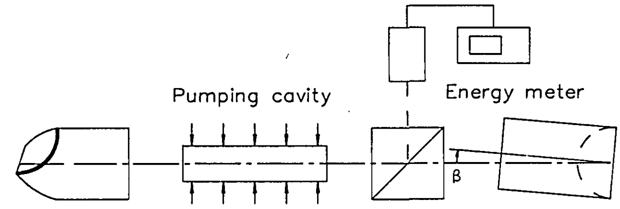

Fig. 8. Experimental setup to measure the alignment tolerance in the horizontal direction.

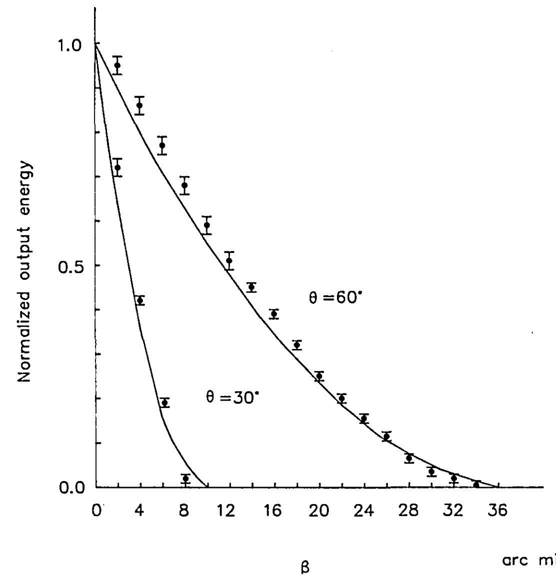

Fig. 9. Normalized output energy vs horizontal misalignment angle.

The results are plotted in Fig. 9, in which the solid lines represent the theoretical calculations from Eq. (7) and the dots are the average values of the measured data. The error bars represent total data spread of measurements. The pulse energies are measured by an ILS model LEM-1-PE energy meter. The misaligned angles are measured by an angular encoder (Physik Instrumente Co.) which has an angular resolution of 1 sec of arc. A reduction in the output energy due to horizontal misalignment is seen. Obviously, energy degradation is more serious at smaller azimuth angles. Thus, the alignment tolerance of the resonator at small azimuth angles are smaller than those at larger azimuth angles.

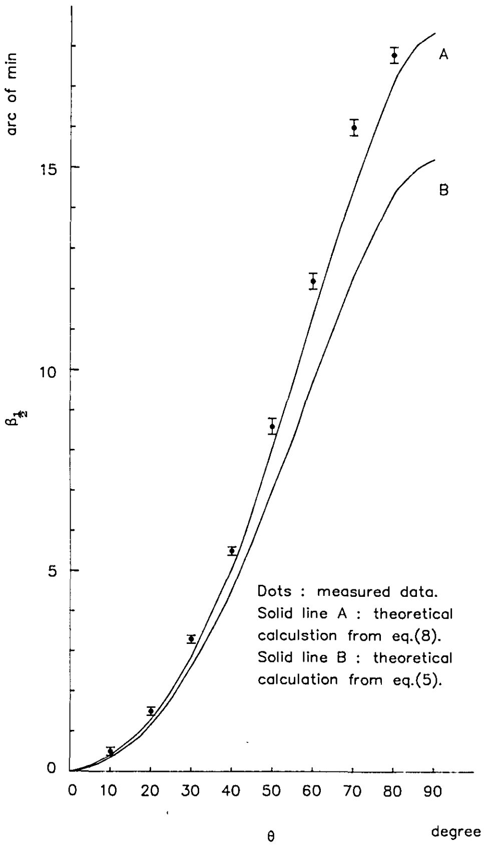

Fig. 10. Horizontal angular alignment tolerance vs the prism azimuth angle.

More data are taken for other prism azimuth angles. The alignment tolerance vs the azimuth angle is plotted in Fig. 10 in which the lower solid line represents the theoretical calculation using Eq. (5), the upper solid line represents the theoretical result using Eq. (8), and the dots are the measured data. The parameters used here are L = 266 mm, L_2 = 165 mm, a = 2.5 mm, d = 64 mm, and n = 1.82. The laser was operated at multimode in all these measurements.

To verify our theoretical prediction on mode area reduction, we have taken the beam spots on a piece of thermal paper placed at 60 cm from the beam splitter (see Table I). The shrinkage of mode area as a function of tilt angle is clearly seen. By comparing the

Table I. Mode Patterns Recorded on a Slip of Thermal Paper Placed 60 cm from the Beam Splitter ($\theta = 60°$)

β (arc min)	Mode pattern	Diameter (mm)	Normalized spot area	Normalized output energy
0		4.3	1.00	1.00
1		4.3	1.00	0.98
2		4.2	0.95	0.95
3		4.1	0.91	0.90
4		4.0	0.86	0.86
5		3.9	0.82	0.82
6		3.8	0.78	0.77
7		3.7	0.74	0.73
8		3.6	0.70	0.68

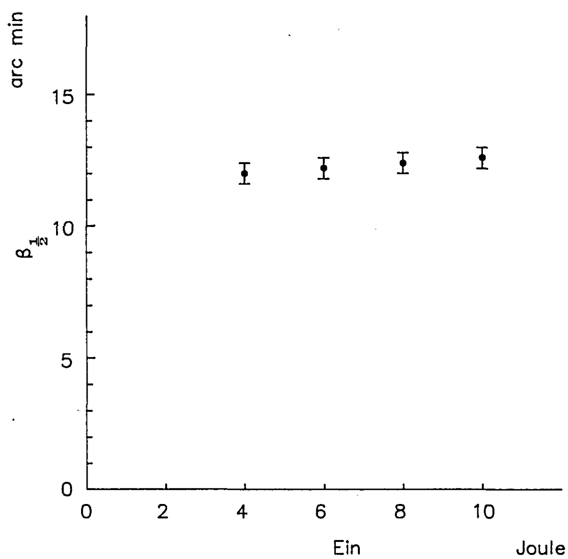

Fig. 11. Horizontal angular alignment tolerance vs pumping energy, when θ = 60°.

normalized spot area with the normalized output energy, these two measured values are very close. This experimental result justifies our assumption that the output reduction at a fixed pumping level is proportional to the mode volume reduction.

We have also examined the dependence of the resonator alignment tolerance on the laser pumping level E_{in}. The results are plotted in Fig. 11. The alignment tolerance is found to be constant within 5% over a range of input energies from 4 to 10 J. The Nd concentration of the rod used here is 1.1%.

The alignment tolerance in the vertical (x) direction was also measured. The same experimental setup shown in Fig. 8 is used except that a stage tiltable vertically replaces the rotary stage. The same experimental procedure is repeated. The output energy is observed to fall very slowly when the vertical misalignment increases as shown in Fig. 12, indicating that the resonator is much more stable in the vertical direction than in the horizontal direction. Figure 13 shows the measured alignment tolerance in the vertical direction vs the prism azimuth angle.

IV. Discussion and Conclusion

The misalignment sensitivity of a Porro prism laser resonator has been analyzed using the ray optics approach by a calculation of the mode volume reduction. Analytical expressions for the normalized output energy and the alignment tolerance are obtained. They predict that the laser output energy decreases as the misalignment angle β increases, and the decaying rate strongly dependes on the prism azimuth angle θ. Output reduction is much more rapid at smaller azimuth angles, showing that the Porro prism resonator is more stable at higher azimuth angles. Theory also predicts that angular alignment tolerance in the horizontal direction depends on resonator length L, rod diameter $2a$, and rod location L_2 according to Eq. (5). Larger L and L_2, and smaller a will give smaller tolerance.

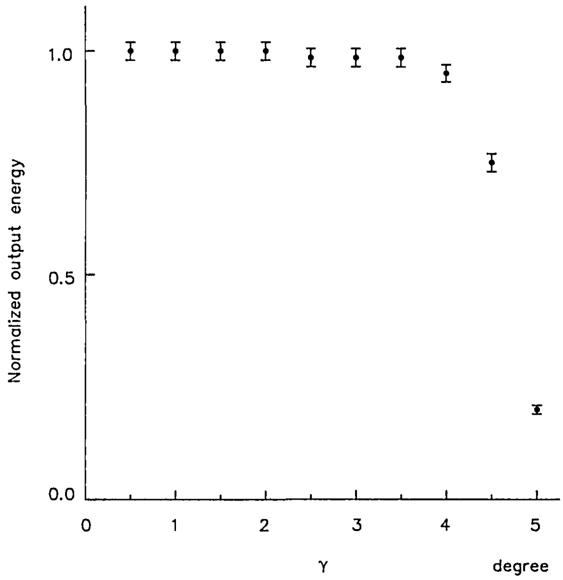

Fig. 12. Normalized output energy vs the vertical misalignment angle, when $\theta = 70°$.

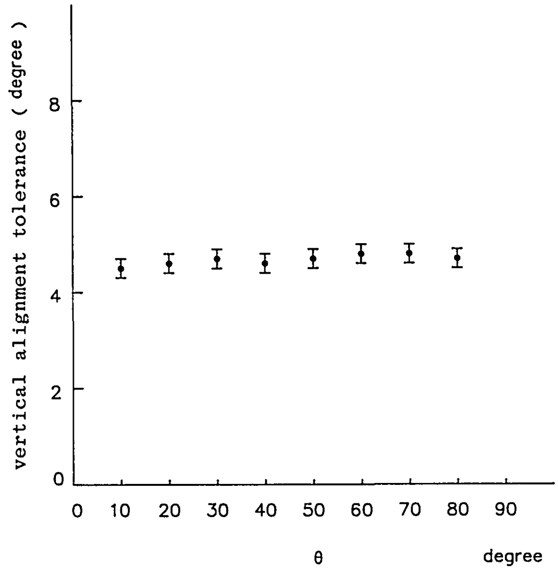

Fig. 13. Vertical angular alignment tolerance vs the prism azimuth angle.

Small angle approximation and uniform photon density assumption has been made in our theory. However, the experimental data (Figs. 9 and 10) are in good agreement with theoretical predictions. It is clear from these results that the largest alignment tolerance occurs when $\theta = 90°$. The dependence on the input energy was also experimentally investigated. The measured alignment tolerance (Fig. 11) is found to be constant within 5% over the range of pumping energies used.

When prism 2 is tilted in the vertical (x) direction, theory predicts that, due to the retroreflecting property of the Porro prisms, it does not cause output energy reduction. This is proved experimentally (see Fig. 12). There is a rapid drop in output energies when vertical misalignment angle (γ) exceeds 4 degrees. This happens because the incident angle at one of the roof surfaces is no longer larger than the critical angle (θ_c) required for total internal reflection (TIR). For example, when refractive index = 1.516, the critical angle for TIR is 41.3°. When the prisms are optimally aligned, the incident angle of the oscillating rays parallel to the z-axis at the roof surfaces is 45°. Therefore, when $\gamma > 3.7°$, the incident angle of the oscillating rays becomes smaller than θ_c, TIR is destroyed and laser action ceases.

It should be noted that the mode axis may not exist when the line $\overline{P'Q'}$ shown in Fig. 3 falls beyond the limits defined by the finite lateral sizes of the apertures of the end reflectors and the laser rod. Consequently we can also theoretically estimate the cutoff angle of misalignment at which laser action ceases. In our case, the laser rod provides the limiting apertures. By putting $\Delta_3 = a$ [Eq. (2)] into Eq. (6), we can predict the cutoff misalignment angle. When $\theta = 60°$ and 30°, the cutoff angles are 36 arc min and 10 arc min, respectively; these are in good agreement with experiment (see Fig. 9).

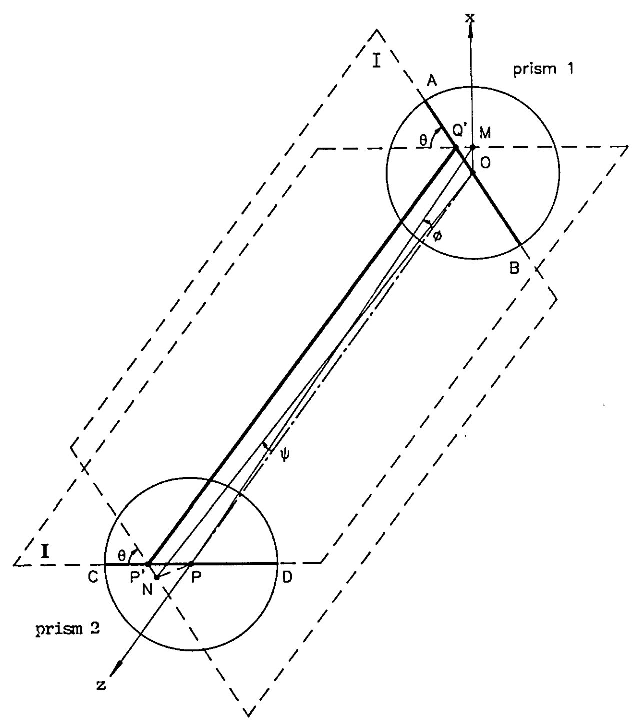

Fig. 14. Illustration of the apex planes tilting due to horizontal misalignment.

In this paper, only the angular tilting of one end prism is considered. However, the method can be used to analyze the misalignment sensitivity in a more general situation (e.g., both prisms are tilted in both directions). Although our experiment was performed using a Nd:YAG laser oscillator, the conclusions should be applicable to other lasers.

The authors wish to thank C. T. Fang and I. C. Kuo for their helpful comments on the original manuscript.

Appendix: Apex Plane Tilting Due to Horizontal Angular Misalignment

The tilting angles of the apex planes due to the horizontal misalignment are denoted as ψ and ϕ for I and II, respectively, which are illustrated in Fig. 14. According to the geometric relationship, ψ and ϕ can be written as

$$\begin{aligned} \psi &\cong \arctan\left(\frac{\overline{PN}}{L}\right), \\ \phi &\cong \arctan\left(\frac{\overline{OM}}{L}\right). \end{aligned} \tag{A1}$$

Recalling that the radial shift of the mode axis reported in the previous paper,[5] we get

$$\begin{aligned} \overline{PN} &= \overline{PP'} \sin\theta \cong (L\beta \csc^2\theta) \sin\theta = L\beta \csc\theta, \\ \overline{OM} &= \overline{OQ'} \sin\theta \cong (L\beta \cot\theta \csc\theta) \sin\theta = L\beta \cot\theta. \end{aligned} \tag{A2}$$

Putting Eq. (A2) into Eq. (A1), we obtain

$$\begin{aligned} \psi &\cong \arctan(\beta \csc\theta) \cong \beta \csc\theta, \\ \phi &\cong \arctan(\beta \cot\theta) \cong \beta \cot\theta. \end{aligned} \tag{A3}$$

References

1. M. K. Chun and E. A. Teppo, "Laser Resonator: an Electrooptically Q-Switched Porro Prism Device," Appl. Opt. **15**, 1942–1946 (1976).
2. G. Zhou and L. W. Casperson, "Modes of a Laser Resonator with a Retroreflecting Roof Mirror," Appl. Opt. **20**, 3542–3546 (1981).
3. G. Gould, S. Jacobs, P. Rabinowitz, and T. Shultz, "Crossed Roof Prism Interferometer," Appl. Opt. **1**, 533–534 (1962).
4. J. F. Lee and C. Y. Leung, "Beam Pointing Direction Changes in a Misaligned Porro Prism Resonator," Appl. Opt. **27**, 2701–2707 (1988).
5. J. F. Lee and C. Y. Leung, "Lateral Displacement of the Mode Axis in a Misaligned Porro Prism Resonator," Submitted to Applied Optics for publication.
6. R. J. Freiberg and A. S. Halsted, "Properties of Low Order Transverse Modes in Argon Ion Lasers," Appl. Opt. **8**, 355–362 (1969).
7. I. C. Kuo and T. Ko, "Laser Resonators of a Mirror and Corner Cube Reflector: Analysis by Imaging Method," Appl. Opt. **23**, 53–56 (1984).
8. T. C. Hsieh, K. Y. Hsu, and Y. J. Li, "Misaligned Spherical-Mirror Waveguide Resonators," Jpn. J. Appl. Phys. **25**, 6–00 (1986).

Moonrocks show rare mineral. A new type of rock, revealing information about a little-understood layer of the lunar crust, was identified recently from rock samples brought back from the moon 20 years ago by Apollo 15 astronauts. An ultra-thin slice of lunar breccia, bits of soil and rocks fused together by heat generated from meteor impacts, revealed mostly feldspar, olivine and spinel, as well as several well-defined crystals of magnesium cordierite, an extremely rare mineral found in metamorphic rocks. According to Ursula B. Marvin at the Harvard-Smithsonian Center for Astrophysics, who made the discovery, the maximum pressure at which this combination could form is equal to that of about 30 miles below the moon's surface, or about six miles above the crust-mantle boundary. Only a major cataclysm such as a meteorite impact could have exposed it to view, Marvin says.